NASA TN D-1200

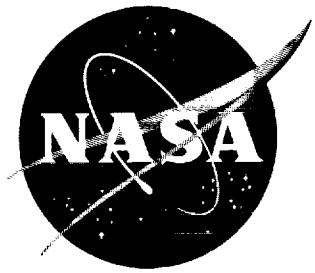

TECHNICAL NOTE

D-1200

EXPERIMENTAL INVESTIGATION OF STRESS DISTRIBUTIONS NEAR ABRUPT CHANGE IN WALL THICKNESS IN THIN-WALLED PRESSURIZED CYLINDERS

By William C. Morgan and Peter T. Bizon

Lewis Research Center
Cleveland, Ohio

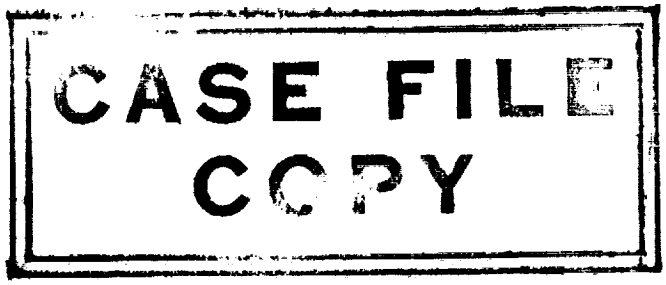

NATIONAL AERONAUTICS AND SPACE ADMINISTRATION

WASHINGTON

June 1962

NATIONAL AERONAUTICS AND SPACE ADMINISTRATION

TECHNICAL NOTE D-1200

EXPERIMENTAL INVESTIGATION OF STRESS DISTRIBUTIONS NEAR ABRUPT CHANGE IN WALL THICKNESS IN THIN-WALLED PRESSURIZED CYLINDERS

By William C. Morgan and Peter T. Bizon

SUMMARY

An experimental investigation was made (1) to evaluate previously published theoretical procedures for the prediction of stress distribution for cases of radially symmetric abrupt change in wall thickness of thin-walled cylinders subject to internal pressure and (2) to investigate the significance of stresses attributable to the presence of thickness changes typical of design practice. One theory was adequate in itself for solution of the case of continuous middle surface; use of the second theoretical procedure was required to determine the additional stresses arising from discontinuous middle surfaces at the change in thickness.

Comparisons were made between theoretical and experimental stress distributions for cases with continuous middle and continuous inner surfaces for radially symmetric changes in wall thickness of a cylinder subject to internal pressure for diameter to larger wall thickness ratios of 117 and 28 and for the case of a continuous outer surface for a ratio of 28. In all tests the ratio of wall thicknesses at the change in wall thickness was 0.4.

There was reasonably good correlation between theoretical and experimental curves of stress distribution. On the basis of this correlation, it was concluded that the applicable theories were valid. It was shown that inclusion of the stresses arising from the condition of discontinuous middle surfaces at a change in thickness has an important effect on stress distribution.

In the case of a cylinder with a continuous outer surface, the maximum mean effective stress was of sufficient magnitude to indicate that this geometry should be avoided in design if possible. The maximum mean effective stress was not increased to a significant degree by the presence of a change in wall thickness in the other cases.

INTRODUCTION

An experimental investigation was made (1) to evaluate previously published theoretical procedures for prediction of elastic stress distributions for two general cases of radially symmetric abrupt change in wall thickness of thin-walled cylinders subject to internal pressure and (2) to investigate the qualitative significance of additional stresses attributable to the presence of changes in wall thickness typical of design practice. The two general cases were characterized by continuous or discontinuous middle surfaces. In this report, middle surface will be defined as the surface generated by a meridian midway through the wall thickness of a cylindrical section.

The methods of analysis were obtained from a recent study of theoretical stress distributions arising from wall discontinuities in shell-type structures typical of space-vehicle design (ref. 1). The case for a continuous middle surface has been described in another analytical investigation (ref. 2), but a search of the literature indicated that the analysis presented in reference 1 for the case of a discontinuous middle surface apparently has not been considered in previously published analyses. In the theoretical solutions, a number of factors were neglected, among them the effect of stress concentration at the change in thickness, the effect of fillets, and the absence of perfect radial symmetry.

The principal purposes of the present investigation were to provide experimental verification of the theoretical analyses and to determine whether simplifying assumptions with regard to the cylinder geometry would cause significant disparity between predicted and experimentally measured stress distributions. The scope of the investigation included tests of cylinders with continuous and discontinuous middle surfaces for nominal ratios of diameter to larger wall thickness of 117 and 28.

In the test cylinder with the ratio of 117 there were fillets at changes in wall thickness. In addition, the cylinder was slightly out of round, and the method of fabrication required the presence of a longitudinal joint reinforcement. The cylinders with the lower ratio of diameter to larger wall thickness were made more in accordance with the assumptions of the theoretical analyses. The changes in wall thickness were not provided with fillets, and cylinder diameters were held to within ±0.001 inch. The ratio between cylinder wall thicknesses at a change in thickness was 0.4 for all the test cylinders.

Three conditions of wall thickness change were investigated: continuous middle surface, with material removed in equal amounts from the inner and outer walls to form the thin section; discontinuous middle surface, with material removed only from the outer surface and with a continuous inner surface; and a second case of discontinuous middle

surface, with material removed only from the inner surface and with a continuous outer surface. Experimental stress distributions were determined from strain data obtained with bonded electrical resistance foil gages.

THEORETICAL STRESS DISTRIBUTION

The basic theoretical analyses are described in reference 1. The original equations were modified slightly for the specific purpose of the present investigation. A list of symbols and subscripts appears in appendix A, and the modification of the analysis is presented in appendix B. Figure 1 shows the notation and sign convention involved in the theoretical procedure.

In the initial part of the calculation, the membrane stresses attributable to pressure were found with the cylinder sections on each side of the change in wall thickness treated as separate simple cylinders. In order to complete the solution, the shears and moments that arose at the change in wall thickness because of the difference in radial expansion between the cylinder sections were treated as edge loads on unpressurized cylinders, and the resulting stresses were superimposed on the membrane stresses.

The difference between the radii of the cylinder middle surfaces on each side of the change in wall thickness was considered as creating additional shears and moments acting as edge loads. In principle, the sum of the stresses would include the membrane stresses, the stresses attributable to difference in radial expansion at the change in wall thickness, and the stresses caused by the difference between middle-surface radii. In the actual calculation, however, it was more expedient to determine the shears and moments present because of the discontinuous middle surface and to combine them with the shears and moments resulting from differential expansion. The complete solution then was obtained by means of the principle of superposition.

EXPERIMENTAL EQUIPMENT AND PROCEDURE

The tests were made for nominal ratios of diameter to maximum wall thickness of 117 and 28. The cylinders and the experimental equipment are described in this section together with the procedure followed in obtaining and reducing the data.

Large Cylinder

The geometry of the larger cylindrical shell is given in figure 2. The cylinder was made from a single sheet of 6061-0 aluminum rolled to shape and welded along the longitudinal seam. Flanges were attached by welding for installation in the test facility, and the complete assembly was heat-treated to the T-6 condition.

Changes in cylinder wall thickness for the cases of continuous middle surface and continuous inner surface were obtained by chemical milling subsequent to heat treatment. Transitions between sections of different thickness had fillet radii approximately the same as the depth of milling. The thin-walled sections were not circumferentially uniform because of the presence of the longitudinal weld.

The cylinder was not perfectly round, and the weld seam was an additional variation from the theoretical assumption of radial symmetry. These factors were considered in selection of strain-gage locations. Outside diameters were measured at four axial locations at intervals of $22\frac{1}{2}^{\circ}$ around the cylinder with no internal pressure. The measurements were repeated at a pressure of 50 pounds per square inch within the cylinder. The variation of diameters from average was found for both pressure levels. On the basis of these data, a meridian was selected in a part of the cylinder that appeared most nearly to conform to a circular arc over approximately 45°, had fairly constant variation from average diameter, and was remote from the weld.

The locations of strain gages along the meridian are shown in figure 3(a). Two strain gages were mounted at each point, one oriented meridionally, the other circumferentially, as close to the meridian as physical size of the gages would permit. Similar gage installations were made on the interior and exterior surfaces. Strain gages for the inner wall were mounted first. Radiographs then were made that showed gage locations with reference to triangular lead foil markers on the outer surface. The radiographs were used as templates for locating gages on the outside of the cylinder. Figure 4 shows the final installation on the exterior surface. Additional axially oriented gages were mounted in areas of membrane stress on the outer surface. The locations of these gages are shown in figure 5, together with the location of the meridian along which the biaxial strain measurements were made.

The cylinder was installed in the facility shown in figure 6. Lead wires from the inner-surface gages were brought out through a bulkhead fitting in the lower head of the test cylinder. During the test a protective cover was lowered over the facility.

Small Cylinders

The geometries of the three small cylinders made for the experimental investigation are given in figure 7. The discontinuities were abrupt, with minimum fillet radii at the transitions; this condition is in accordance with theoretical assumptions. These cylinders were machined from 2014-T6 extruded aluminum tubing and provided with heads of the type shown in figure 8. These end closures have been found satisfactory for relatively high pressure operation. Assembly and disassembly were effected by bringing the parts to a temperature within the melting rage of the alloy that forms the seal.

The locations of strain gages on the inner and outer surfaces along a meridian are shown in figure 3(b). Two gages oriented to measure the principal biaxial strains were installed at each point, and the inner and outer gages were mounted in as near the same locations as possible by the use of radiograph templates, as previously described. Selection of meridians for locating the strain gages on the three small cylinders was arbitrary, as there were no radial discontinuities and preliminary diameter measurements indicated that the cylinders were true to within ±0.001 inch. Figure 9 shows a typical strain-gage installation on the outer surface of a cylinder ready for testing. Reference is made to figure 8 for the method of bringing out the lead wires from the strain gages inside the cylinder.

Testing Equipment and Procedure

The strain measurements were made with 120-ohm electrical-resistance bonded foil strain gages. The gages were mounted with cyanoacrylate cement. In the case of the three small cylinders, gages with 1/16-inch effective length were used throughout, and in the installation for the larger cylinder these gages were used in regions where steep stress gradients could be expected to occur or where physical limitation of area made it advisable. Gages with elements 1/8 inch in length were used elsewhere.

The strain-gage lead wires were brought to a terminal box near the facility and connected through a five-wire system to a multichannel digital strain recorder in an adjacent control room. This equipment, used for balancing, calibrating, controlling, scanning, and recording the strain-gage output, was accurate to ±1.0 percent of strain-gage output. The output was recorded automatically on both a typed record and a punched paper tape.

Internal pressure to the test cylinders was supplied by a hydraulic system. The pressure gages used in the experiment were calibrated and found to have a maximum error of less than 0.5 pound per square inch.

The test procedure consisted of raising the internal pressure to a predetermined value and returning to zero pressure. The basic cycle was repeated for progressively higher pressures until a predetermined maximum had been reached. The purpose of making successive increases in pressure was to provide data for correction of any nonlinearity in strain-gage output. Data were recorded at every pressure level.

Data were obtained for the larger cylinder at pressures of 100, 110, 120, 130, 140, and 150 pounds per square inch and for the three smaller cylinders at 200, 300, 400, 500, 600, and 621 pounds per square inch. The level of maximum stress was approximately the same for all the test cylinders.

A computer program was prepared for reduction of the data. This program read in the data from duplicate tests, corrected for zero drift, corrected for nonlinearity using the method of least squares, averaged strains from the two tests, and converted these strains to stresses using the following relations:

Meridional stress

$$\sigma_x = \frac{E}{1 - \nu^2} (\epsilon_x + \nu\epsilon_\theta) \qquad (1)$$

Circumferential stress

$$\sigma_\theta = \frac{E}{1 - \nu^2} (\epsilon_\theta + \nu\epsilon_x) \qquad (2)$$

RESULTS AND DISCUSSION

Upon completion of the tests, the experimental results were compared with the theoretically predicted stress distributions for the maximum test pressures.

Large Cylinder

The presence of the longitudinal weld was a departure from the condition of radial symmetry in the thin sections, and the presence of fillets at the changes in thickness was not in agreement with the assumption of abrupt thickness change. In addition, measurements and observations made prior to and during the tests indicated that the cylinder also had imperfections. Figure 10 shows the results of diameter measurements made at internal pressures of 0 and 50 pounds per square inch. The divergence from average diameter was of the order of 1 percent, and the

figure indicates that pressure-dependent changes may occur. Figure 11 shows meridional strain data obtained during the tests in areas of membrane stress, at locations described previously (fig. 5). These data indicate a lack of uniformity that may have been caused by variations in meridional elements or possibly by thickness variation.

The comparison between the predicted and experimental stress distribution for the region with continuous middle surface appears in figure 12; the comparison for the case of continuous inner surface is shown in figure 13.

There appeared to be general qualitative agreement between the theoretical and experimental curves for stress distribution for the case of continuous middle surface (fig. 12). For both inner and outer surfaces, the experimental stresses were equal to or greater than the predicted values, except for the distribution of the circumferential stress on the inner surface, where experimental values were always lower.

In the case of discontinuous middle surface with continuous inner wall, the results of the experimental investigation showed fair qualitative correlation with predicted curves of stress distribution (fig. 13). Measured circumferential stresses generally were low, except at the outer wall of the thick section of the cylinder. The experimental meridional stresses in the inner wall were low for the most part. Observed values of stress for meridional distribution in the outer surface were higher than theoretical, except for three points near the membrane area of the thin section.

Small Cylinders

The results obtained from the tests of the small cylinders, together with the predicted stress distributions, are presented in figures 14, 15, and 16, for the cases of continuous middle surface, continuous inner surface, and continuous outer surface, respectively.

Curves faired through the experimental results indicated good qualitative correlations, and the meridional stress data showed good agreement with the values predicted by theory for the small cylinder with continuous middle surface (fig. 14). The experimental results for circumferential stress distributions were found to be low, however, except for the inner wall of the thicker cylinder section, for which the measured predicted curves were nearly coincident.

The curves obtained by experiment for the case of continuous inner surface were nearly similar in shape to the curves predicted by theory, providing reasonable qualitative correlation (fig. 15). The actual stress

distributions generally were somewhat lower than predicted, except for the meridional stresses in the inner wall of the thin section and the outer wall of the thicker section close to the change in thickness.

Curves of stress distribution for meridional and inner-surface circumferential stresses showed good correlation between observed and predicted values in the case of continuous outer surface (fig. 16). Quantitative agreement was not as close for outer-surface circumferential stress distribution, but the shapes of the theoretical and experimental curves were nearly the same.

The geometry of the small cylinders conformed closely to the theoretical assumptions, with the exception that the ratio of diameter to larger wall thickness of 28, for the small-cylinder tests, was near the lower limit for application of analysis based on thin-wall theory. It was decided to determine the change in predicted stress distribution that would result if these cylinders were considered as thick-walled. It was found that the membrane stresses would be changed to an appreciable extent, but the effect would not be as great in the calculation of shears and moments arising from change in wall thickness. A more detailed discussion appears in appendix C.

Comparisons between the experimental results and stress distributions determined by this modified calculation are presented in figures 17, 18, and 19 for the cases of continuous middle surface, continuous inner surface, and continuous outer surface, respectively. In general, there appeared to be a slightly better correlation. The major effect appeared to be a change in the curves of circumferential stress distribution.

Discussion

This section of the report presents a more general review of the results already discussed briefly. In all cases, there appeared to be reasonable qualitative correlation between theoretical and experimental curves of stress distribution, indicating the presence of virtually constant errors in the data. The most marked examples of discrepancy may be found in the curves for circumferential stress. The experimental results were low, with the single exception of the curve for outer-surface circumferential stress in the thin section of the large cylinder with a continuous middle surface (fig. 12). There was no readily apparent explanation for this variation between predicted and observed stress distributions. The possibility exists that there may have been some end effect, although a prior analysis indicated that this factor should be negligible.

Average magnitudes of percent variations, meridional and circumferential, for each case of change in wall thickness and for all cylinders are presented in table I. An examination of the table indicates that maximum variation occurred most frequently for measurements in the outer surface. The most marked effect of the small-cylinder modified calculation was a decrease in variation for outer-surface circumferential stresses.

Table II presents a comparison of magnitudes of overall percent variation. Maximum average variation occurred in the results obtained from the large-cylinder tests. Using thick-wall equations for the membrane stresses in the small cylinders produced a general decrease in variation between experimental and predicted stress values.

In the cases of change in wall thickness characterized by continuous middle surface and continuous inner surface, the increases in maximum stress compared to membrane stress were not excessive. In the case of a cylinder with continuous outer surface, however, it appeared that the increase in inner-surface meridional stress might be of considerable importance. Therefore, it was decided to compare the predicted curves of stress distribution in the small cylinders on the basis of effective stress as determined from the von Mises distortion energy theory, because of the present trend in design practice for missile structures to allow stresses close to the yield point. The comparison, based on values obtained from the modified calculations, is presented in figure 20. This comparison shows that there is a significantly higher effective stress in the thin section of the cylinder immediately adjacent to the change in thickness for the case of a continuous outer wall. It is apparent that, if a specific design requires an abrupt change in cylinder wall thickness, material should not be removed from the inner surface only, because of the considerable increase in effective stress level and the decrease in the margin of safety for the specified thickness of material.

In general, it appeared that in the tests made with the larger cylinders the degree of correlation between theoretical and experimental stress distributions was affected to some extent by the presence of fillets at changes in thickness and by the presence of a longitudinal joint reinforcement. It is probable, however, that imperfections such as lack of radial symmetry and meridional variations were more important sources of apparent experimental error. Correlation was somewhat better for the cases of change in wall thickness tested in small cylinders.

SUMMARY OF RESULTS

Comparisons were made between theoretical and experimental stress distributions for cases with continuous middle and continuous inner surfaces for radially symmetric changes in wall thickness of a cylinder

subject to internal pressure for ratios of diameter to larger wall thickness of 117 and 28 and for the case of a continuous outer surface for a ratio of 28. The wall-thickness ratio at the change in wall thickness was 0.4 in all cases.

The degree of correlation established the validity of the analytical procedures, although the larger cylinder was not made in strict accordance with theoretical assumptions and in addition had many imperfections attributable to errors in fabrication. The average variation of experimental results from predicted values of stress was less than 10 percent for all cases, and less than 6 percent for the tests with cylinders for which the fabrication was in close accordance with theoretical assumptions.

It was shown that inclusion of the stresses arising from the condition of discontinuous middle surfaces has an important effect on the prediction of stress distribution. In the case of a cylinder with continuous outer surface, the maximum mean effective stress would be considerably higher, compared to the other cases of change in wall thickness, and this geometry should be avoided in design, if possible. In the other cases considered, the presence of thickness changes did not result in significant increases in maximum mean effective stress.

Lewis Research Center
National Aeronautics and Space Administration
Cleveland, Ohio, January 17, 1962

APPENDIX A

SYMBOLS

a	radius of cylinder, in.
b	mean radius of middle surfaces, $(a_1 + a_2)/2$, in.
c	thickness ratio, h_1/h_2
d	difference in middle surface radii, $a_2 - a_1$, in.
E	modulus of elasticity, psi
h	thickness of cylindrical wall, in.
l	middle surface radius ratio, a_1/a_2
M	bending moment in wall of cylinder, in.-lb/in.
N	axial stress resultant in wall of cylinder, lb/in.
p	uniform internal pressure, lb/sq in.
Q	radial stress resultant in wall of cylinder, lb/in.
x	distance along meridian from discontinuity, in.
β	$\sqrt[4]{3(1 - \nu^2)/a^2h^2}$, in.^{-1}
$\Theta(\beta x)$	$e^{-\beta x} \cos \beta x$
ϵ	strain, in./in.
ν	Poisson's ratio
σ	normal stress, psi
$\Phi(\beta x)$	$e^{-\beta x}(\cos \beta x + \sin \beta x)$
$\Psi(\beta x)$	$e^{-\beta x}(\cos \beta x - \sin \beta x)$
$\Omega(\beta x)$	$e^{-\beta x} \sin \beta x$

Subscripts:

d	discontinuity
i	inner surface

m	membrane
o	outer surface
t	total
x	meridional direction
θ	circumferential direction
0	junction
1	thicker region
2	thinner region

Superscript:

'	denotes thick-wall solution

APPENDIX B

ANALYTICAL DETERMINATION OF STRESSES FOR THIN-WALLED CYLINDER

A sketch of the configuration with a discontinuous middle surface having material removed from the inside is shown in figure 1(a). In order to find the membrane stresses the structure was imagined to be separated at the discontinuity, and each part was treated as a cylinder with closed ends subject to internal pressure. The meridional membrane stresses for the thin and thick sections are

$$\sigma_{x,m,1} = \frac{pa_1}{2h_1} \tag{B1}$$

$$\sigma_{x,m,2} = \frac{pa_2}{2h_2} \tag{B2}$$

and the circumferential membrane stresses are

$$\sigma_{\theta,m,1} = \frac{pa_1}{h_1} \tag{B3}$$

$$\sigma_{\theta,m,2} = \frac{pa_2}{h_2} \tag{B4}$$

In addition to these membrane stresses, discontinuity stresses arise because of the change in thickness and because of the possible discontinuous middle surface at the change in thickness. General equations for the discontinuity forces are presented in reference 1. For a cylindrical shell, these equations reduce to

$$Q_0 = \frac{\frac{2 - \nu}{2\beta_1}\left[(c - 1)(c^{5/2} + 1)\right]}{(c^2 + 1)^2 + 2c^{3/2}(c + 1)} p + \frac{db\beta_2 c^{3/2}(c^{1/2} + 1)}{(c^2 + 1)^2 + 2c^{3/2}(c + 1)} p \tag{B5}$$

$$M_{O,1} = \frac{\frac{2 - \nu}{4\beta_1^2}[(c - 1)(c^2 - 1)]}{(c^2 + 1)^2 + 2c^{3/2}(c + 1)} p - \frac{\frac{dbc^2}{2}(c^2 + 2c^{1/2} + 1)}{(c^2 + 1)^2 + 2c^{3/2}(c + 1)} p \quad \text{(B6)}$$

$$M_{O,2} = \frac{\frac{2 - \nu}{4\beta_1^2}[(c - 1)(c^2 - 1)]}{(c^2 + 1)^2 + 2c^{3/2}(c + 1)} p + \frac{\frac{db}{2}(c^2 + 2c^{3/2} + 1)}{(c^2 + 1)^2 + 2c^{3/2}(c + 1)} p \quad \text{(B7)}$$

where

$$c = \frac{h_1}{h_2} \quad \text{(B8)}$$

and

$$d = a_2 - a_1 \quad \text{(B9)}$$

In these equations the middle-surface-radius ratio is taken equal to unity. A ratio not equal to unity is discussed in appendix C.

If the middle surface is continuous across the thickness change, $a_2 = a_1$ and $d = 0$. Then the second terms in equations (B5) to (B7) drop out and the remainder agrees with the results given for this case in reference 1. It is apparent that the first terms in equations (B5) to (B7) are due to the change in thickness, and the last terms result because the middle surfaces of the two portions of the cylinder are not continuous at the change in thickness. If radius a_2 is less than a_1, d is a negative quantity and the directions of the components of shear and moment due to the discontinuous middle surface will change.

Having determined the discontinuity shear and moment, the discontinuity stresses can be calculated by treating each portion of the shell as a separate cylinder loaded with an edge shear and moment. The sign convention used to compute stresses is that edge shear and moment are positive if they produce outward deflection. Referring to figure 1(b), it can be seen that the assumed direction of the discontinuity shear on the thin section is inward. Therefore, using the sign convention chosen to determine the stresses,

$$Q_{O,1} = -Q_{O,2} = Q_O \quad \text{(B10)}$$

The stresses in a right circular cylinder loaded by edge shear and moment are given in reference 1 as:

Meridional stress

$$\sigma_{x,d,1} = \pm \frac{6}{h_1^2}\left[M_{O,1}\Phi(\beta_1 x) + \frac{1}{\beta_1} Q_{O,1}\Omega(\beta_1 x)\right] \tag{B11}$$

$$\sigma_{x,d,2} = \pm \frac{6}{h_2^2}\left[M_{O,2}\Phi(\beta_2 x) + \frac{1}{\beta_2} Q_{O,2}\Omega(\beta_2 x)\right] \tag{B12}$$

Circumferential stress

$$\sigma_{\theta,d,1} = M_{O,1}\left[\frac{2\beta_1^2 a_1}{h_1}\Psi(\beta_1 x) \pm \frac{6\nu}{h_1^2}\Phi(\beta_1 x)\right] + Q_{O,1}\left[\frac{2\beta_1 a_1}{h_1}\Theta(\beta_1 x) \pm \frac{6\nu}{\beta_1 h_1^2}\Omega(\beta_1 x)\right] \tag{B13}$$

$$\sigma_{\theta,d,2} = M_{O,2}\left[\frac{2\beta_2^2 a_2}{h_2}\Psi(\beta_2 x) \pm \frac{6\nu}{h_2^2}\Phi(\beta_2 x)\right] + Q_{O,2}\left[\frac{2\beta_2 a_2}{h_2}\Theta(\beta_2 x) \pm \frac{6\nu}{\beta_2 h_2^2}\Omega(\beta_2 x)\right] \tag{B14}$$

These stress equations are applicable at any distance x from the loaded edge of the cylinder. Where $\pm$ signs occur, the upper sign refers to the inner surface of the cylinder, and the lower sign refers to the outer surface. In making the computations, values for Θ, Φ, Ψ, and Ω were obtained from the tables of reference 3.

The complete stress distribution for an abrupt change in wall thickness in a thin-walled pressurized structure was found by adding the stresses due to discontinuity to the membrane stresses. Therefore, the complete stress distribution is:

Meridional stress

$$\sigma_{x,t,1} = \sigma_{x,m,1} + \sigma_{x,d,1} \tag{B15}$$

$$\sigma_{x,t,2} = \sigma_{x,m,2} + \sigma_{x,d,2} \tag{B16}$$

Circumferential stress

$$\sigma_{\theta,t,1} = \sigma_{\theta,m,1} + \sigma_{\theta,d,1} \tag{B17}$$

$$\sigma_{\theta,t,2} = \sigma_{\theta,m,2} + \sigma_{\theta,d,2} \tag{B18}$$

APPENDIX C

ANALYTICAL DETERMINATION OF STRESSES FOR MODERATELY THICK-WALLED CYLINDER

The analysis presented in this appendix is not rigorous for thick-walled cylinders. It merely corrects the membrane stresses for the thick-wall effect and gives a more accurate determination of the discontinuity shear and moment by using both middle surface radii rather than an average value.

The cylindrical shell was imagined to be separated at the discontinuity, and each part was treated as a finite-length thick-walled cylinder subjected to internal pressure. The wall stresses for this case are given in reference 4 as:

Meridional stress

$$\sigma'_{x,m,1} = \left(\frac{a_{i,1}^2}{a_{o,1}^2 - a_{i,1}^2}\right)p \tag{C1}$$

$$\sigma'_{x,m,2} = \left(\frac{a_{i,2}^2}{a_{o,2}^2 - a_{i,2}^2}\right)p \tag{C2}$$

Circumferential stress at inner surface

$$\sigma'_{\theta,m,1,i} = \left(\frac{a_{o,1}^2 + a_{i,1}^2}{a_{o,1}^2 - a_{i,1}^2}\right)p \tag{C3}$$

$$\sigma'_{\theta,m,2,i} = \left(\frac{a_{o,2}^2 + a_{i,2}^2}{a_{o,2}^2 - a_{i,2}^2}\right)p \tag{C4}$$

Circumferential stress at outer surface

$$\sigma'_{\theta,m,1,o} = \left(\frac{2a_{i,1}^2}{a_{o,1}^2 - a_{i,1}^2}\right)p \tag{C5}$$

$$\sigma'_{\theta,m,2,o} = \left(\frac{2a_{i,2}^2}{a_{o,2}^2 - a_{i,2}^2}\right)p \tag{C6}$$

The discontinuity shear force and bending moment acting on each part of the shell are determined using the correct middle-surface radius for that part:

$$Q'_{O,d,1} = -Q'_{O,d,2} = \frac{\frac{2-\nu}{2\beta_1}(c - l^2)(c^{5/2}l^{-1/2} + 1)}{(l + c^2)^2 + 2l^{1/2}c^{3/2}(1 + lc)}p$$

$$+ \frac{db\beta_2 c^{3/2}l^{1/2}(1 + c^{1/2}l^{1/2})}{(l + c^2)^2 + 2l^{1/2}c^{3/2}(1 + lc)}p \tag{C7}$$

$$M'_{O,d,1} = \frac{\frac{2-\nu}{4\beta_1^2}(c - l^2)(c^2l^{-1} - 1)}{(l + c^2)^2 + 2l^{1/2}c^{3/2}(1 + lc)}p$$

$$- \frac{\frac{dbc^2}{2}(l + c^2 + 2l^{3/2}c^{1/2})}{(l + c^2)^2 + 2l^{1/2}c^{3/2}(1 + lc)}p \tag{C8}$$

$$M'_{O,d,2} = \frac{\frac{2-\nu}{4\beta_1^2}(c - l^2)(c^2l^{-1} - 1)}{(l + c^2)^2 + 2l^{1/2}c^{3/2}(1 + lc)}p$$

$$+ \frac{\frac{db}{2}(l^2 + lc^2 + 2l^{1/2}c^{3/2})}{(l + c^2)^2 + 2l^{1/2}c^{3/2}(1 + lc)}p \tag{C9}$$

E-1000

If the radius ratio l is taken to be unity, equations (C7) to (C9) reduce to equations (B5) to (B7) previously obtained. In any thin-walled-cylinder problem, such an assumption results in negligible error.

The combined stresses are now found as before using equations (B11) to (B14); however, the primed values for shear and moment are substituted for the unprimed values. Adding the wall stresses found from equations (C1) to (C6) to the discontinuity stresses just obtained gives the complete stress distribution for this case.

REFERENCES

1. Johns, Robert H., and Orange, Thomas W.: Theoretical Elastic Stress Distributions Arising from Discontinuities and Edge Loads in Several Shell-Type Structures. NASA TR R-103, 1961.

2. Timoshenko, S., and Woinowsky-Krieger, S.: Theory of Plates and Shells. Second ed., McGraw-Hill Book Co., Inc., 1959.

3. Hetenyi, M.: Beams on Elastic Foundation. Univ. Mich. Press, 1946.

4. Timoshenko, S.: Strength of Materials. Pt. II. Advanced Theory and Problems. Third ed., D. Van Nostrand Co., Inc., 1957.

TABLE I. - AVERAGES OF MAGNITUDES OF PERCENT VARIATION OF EXPERIMENTAL STRESS FROM THEORETICAL VALUES

	Surface location	Average, from thin-wall calculation		Average, from modified calculation	
		Meridional	Circumferential	Meridional	Circumferential
Large cylinder with continuous middle surface	Inner	5.1	5.9	---	---
	Outer	11.4	4.3	---	---
	Both	8.3	5.1	---	---
Large cylinder with continuous inner surface	Inner	9.0	11.8	---	---
	Outer	19.0	4.0	---	---
	Both	13.8	8.1	---	---
Small cylinder with continuous middle surface	Inner	3.2	2.1	4.0	2.1
	Outer	5.9	10.5	5.2	5.8
	Both	4.5	6.3	4.6	3.9
Small cylinder with continuous inner surface	Inner	4.0	3.9	4.3	2.9
	Outer	9.9	10.9	4.8	5.4
	Both	6.9	7.4	4.5	4.1
Small cylinder with continuous outer surface	Inner	5.8	3.7	4.8	4.0
	Outer	4.0	7.6	4.0	4.6
	Both	4.9	5.6	5.6	4.3

TABLE II. - OVERALL AVERAGES OF MAGNITUDES OF PERCENT VARIATION OF EXPERIMENTAL STRESS FROM THEORETICAL VALUES

	Continuous middle surface	Continuous inner surface	Continuous outer surface	Average
Large cylinder	6.7	10.9	---	8.8
Small cylinders	5.4	5.3	7.2	5.9
Small cylinders, modified calculation	4.3	4.3	5.0	4.6

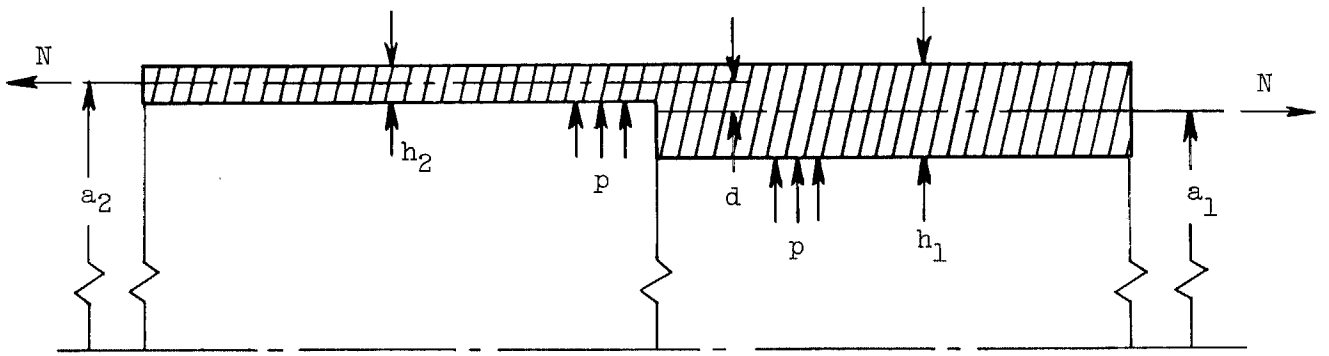

(a) Discontinuous middle surface with material removed from inside.

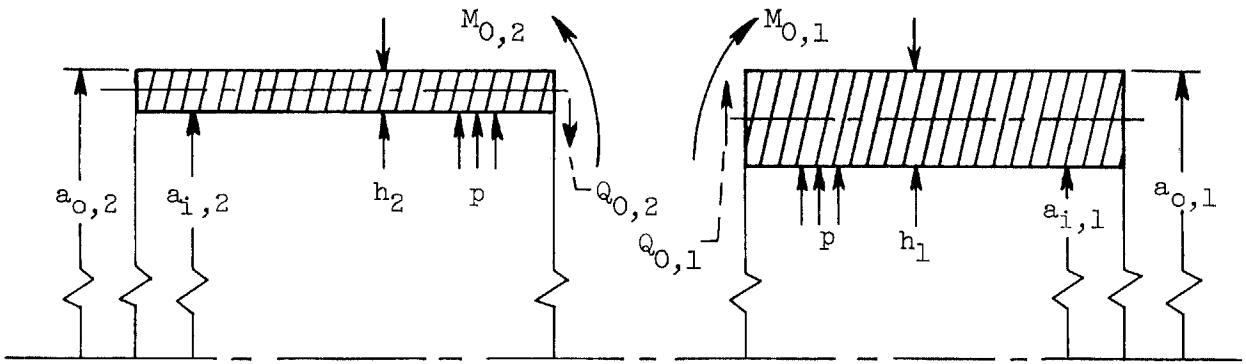

(b) Separate cylinders with edge shear and bending moment and internal pressure.

Figure 1. - Convention for analysis of stress distribution in region of abrupt change in wall thickness of cylindrical pressure vessel.

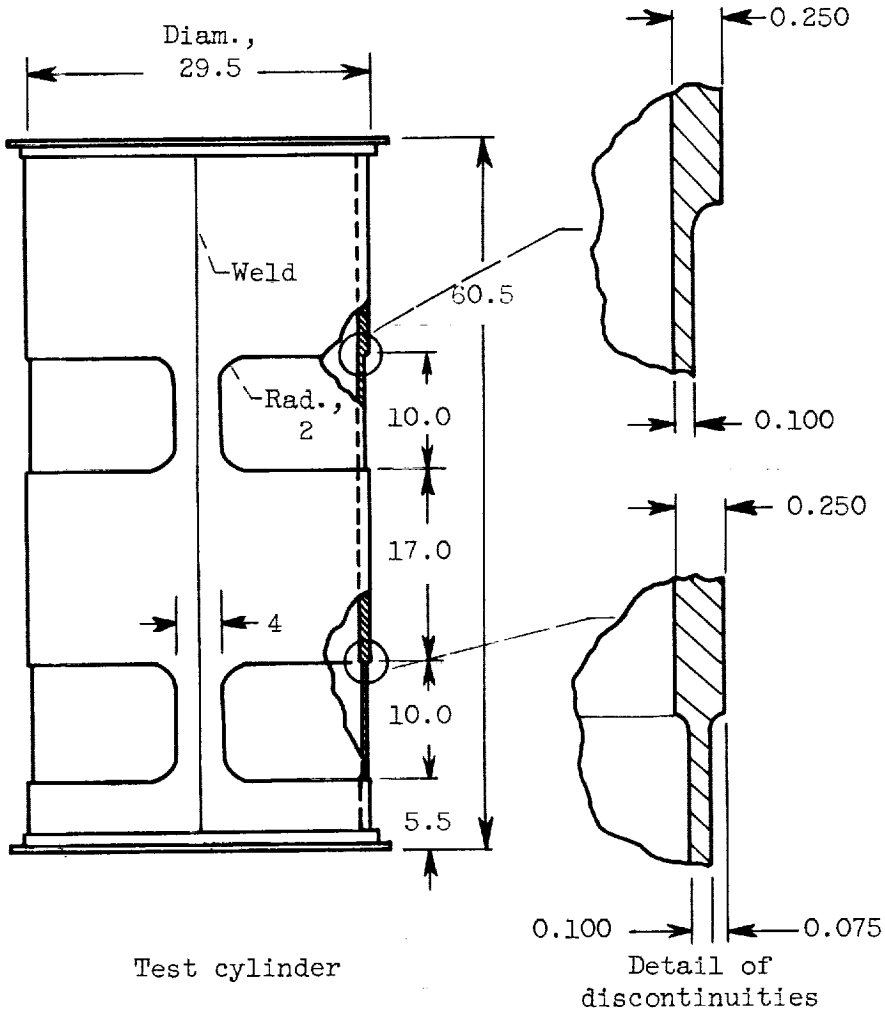

Figure 2. - Geometry of larger cylindrical shell.
(Dimensions in inches.)

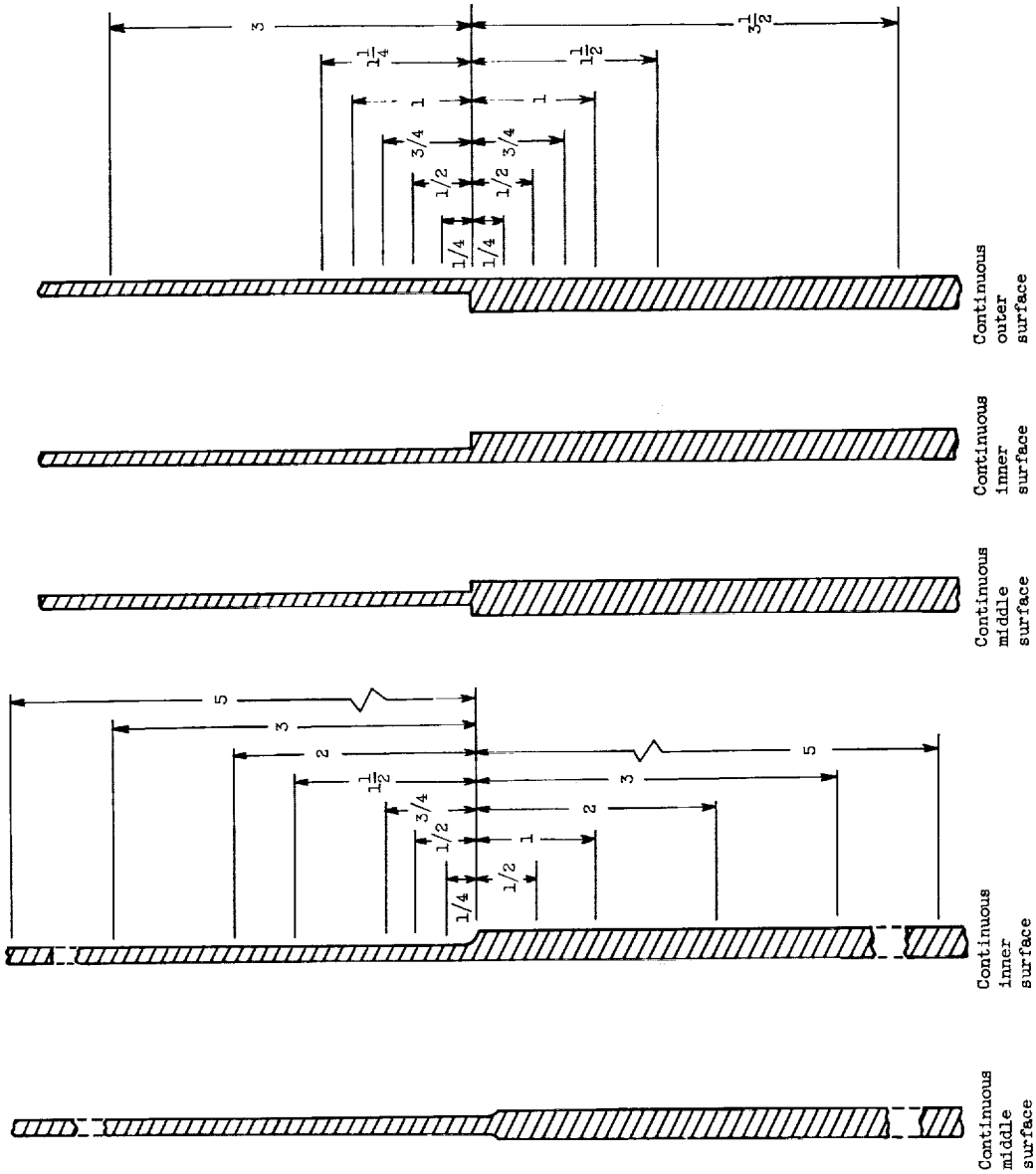

(b) Small cylinders.

(a) Large cylinder.

Figure 3. - Location of perpendicularly oriented strain gages along meridians of test cylinders. (Dimensions in inches.)

Figure 4. - Strain-gage installation on large cylinder.

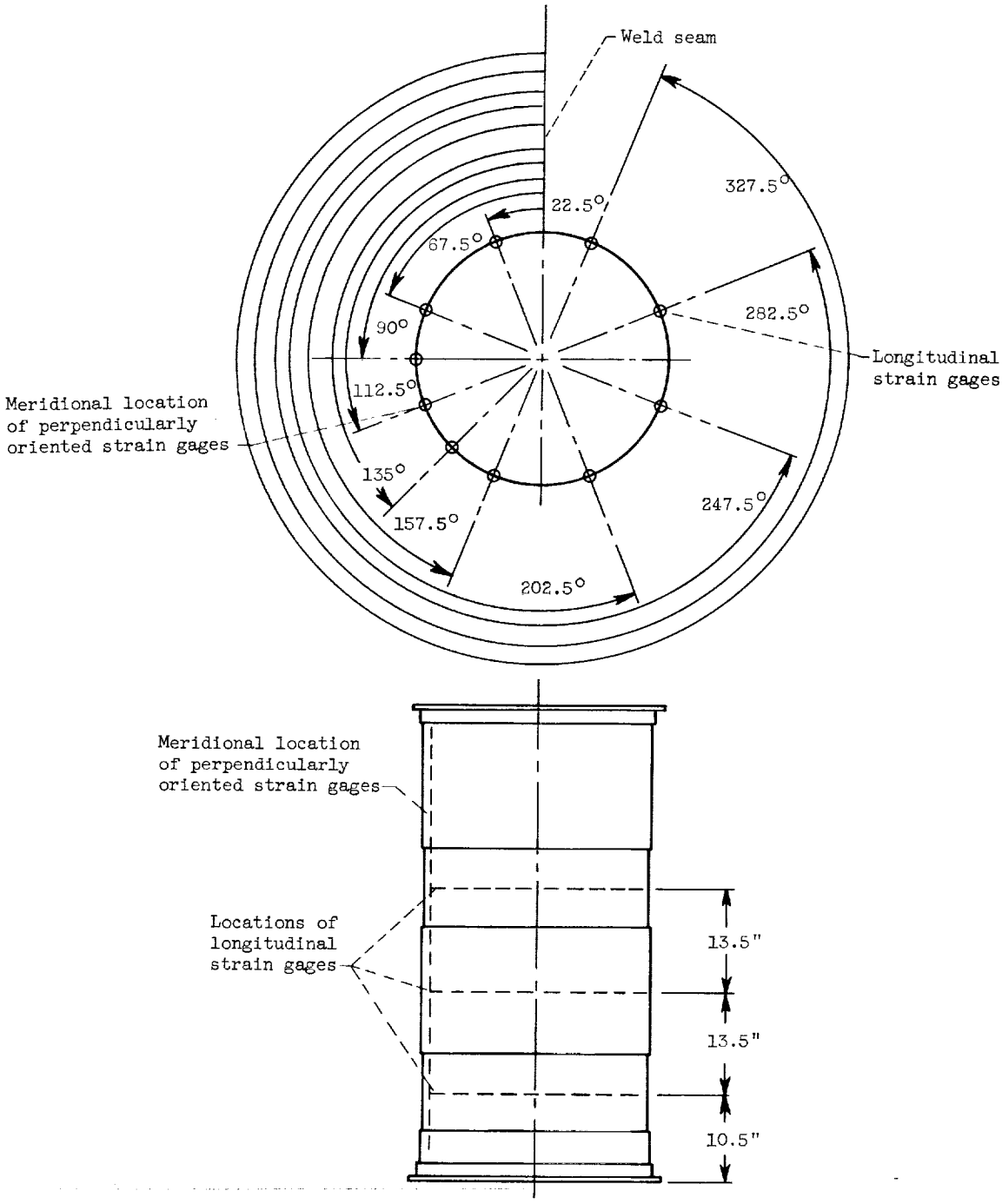

Figure 5. - Location of strain gages used to measure longitudinal membrane strains on outer surface of large cylinder and location of meridian along which biaxial strain measurements were made.

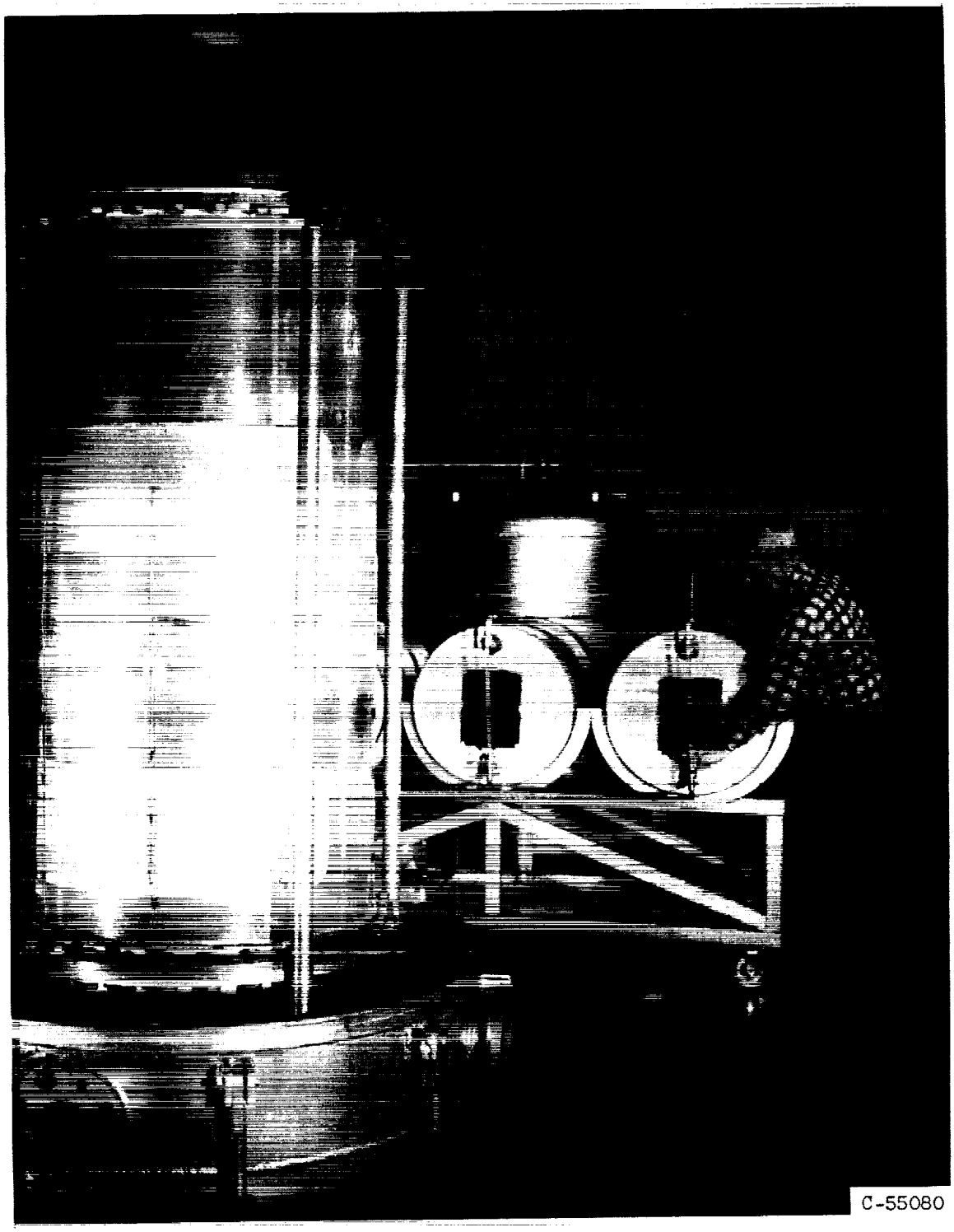

Figure 6. - Test facility with test cylinder installed.

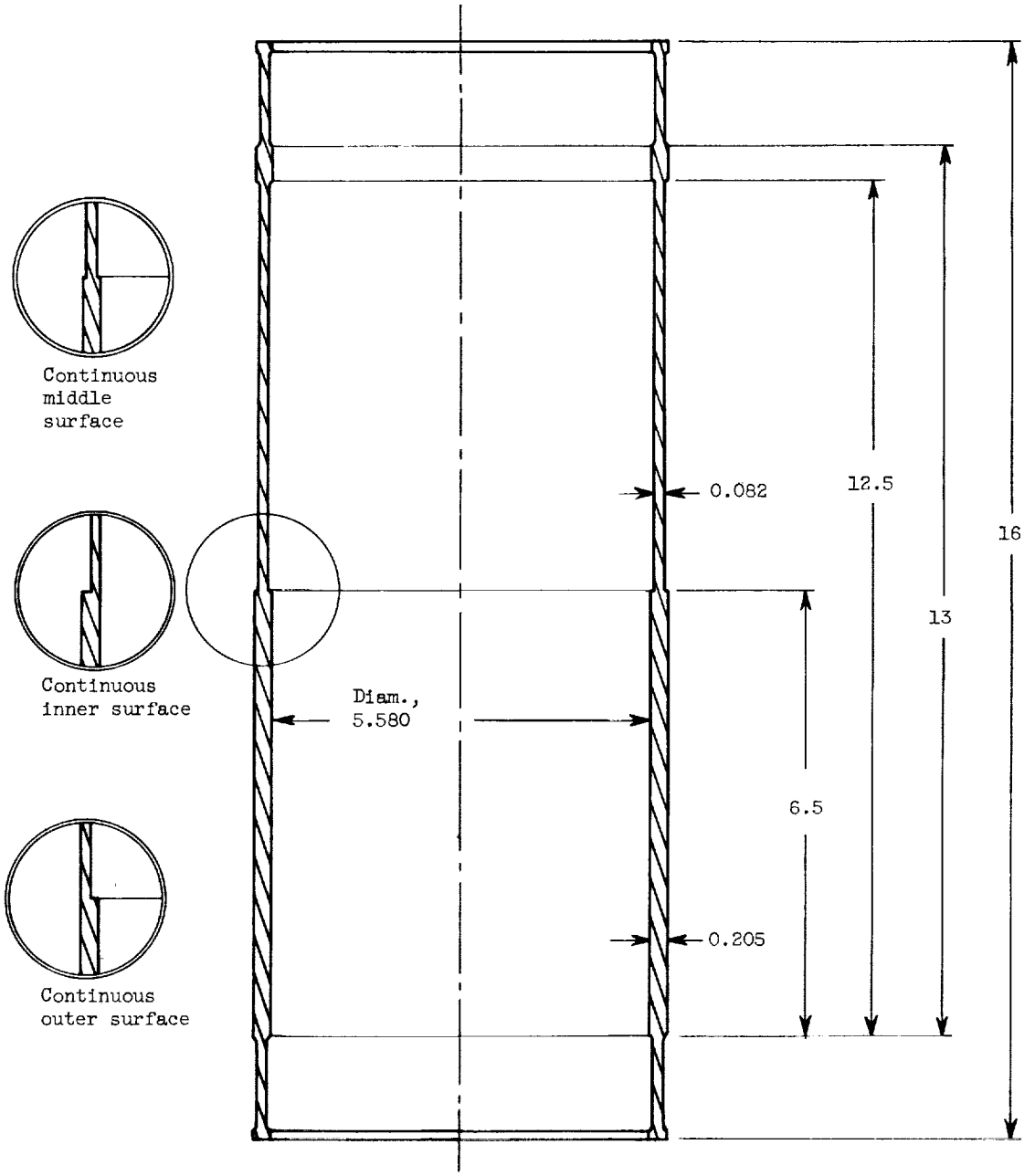

Figure 7. - Geometry of three small cylinders. (Dimensions in inches.)

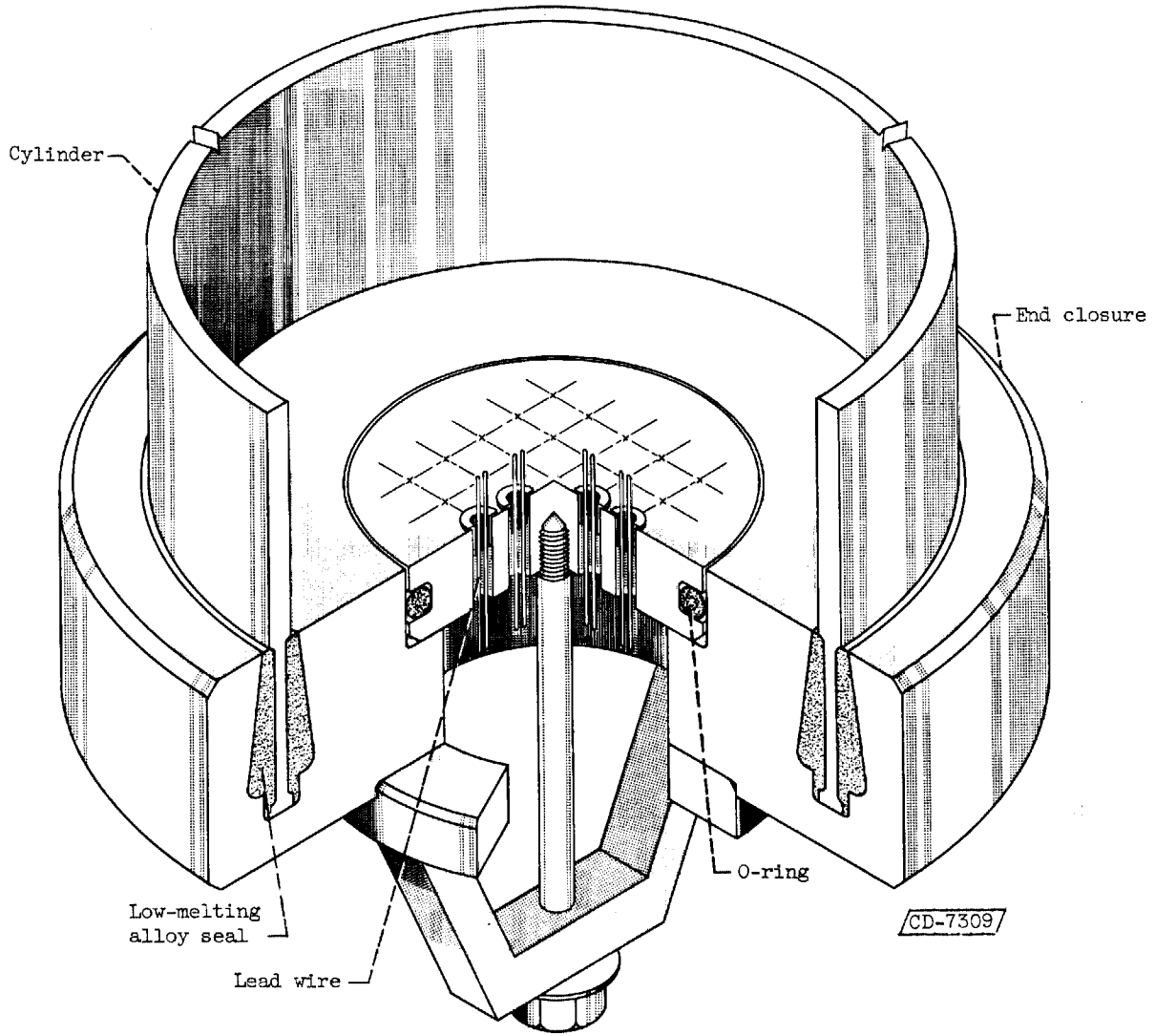

Figure 8. - End closure for small cylinder with provision for bringing out lead wires.

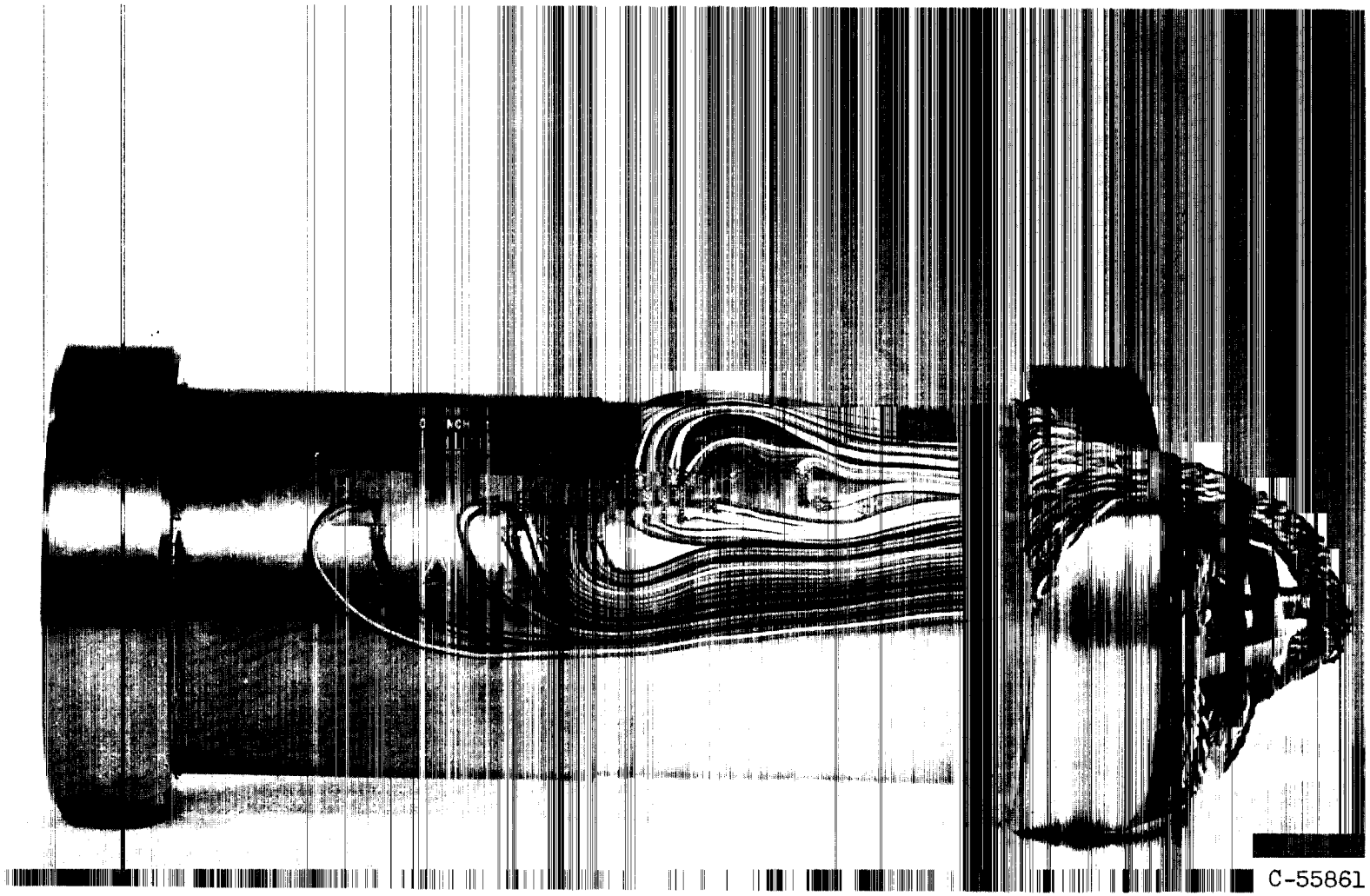

Figure 9. - Strain-gage installation on small cylinder.

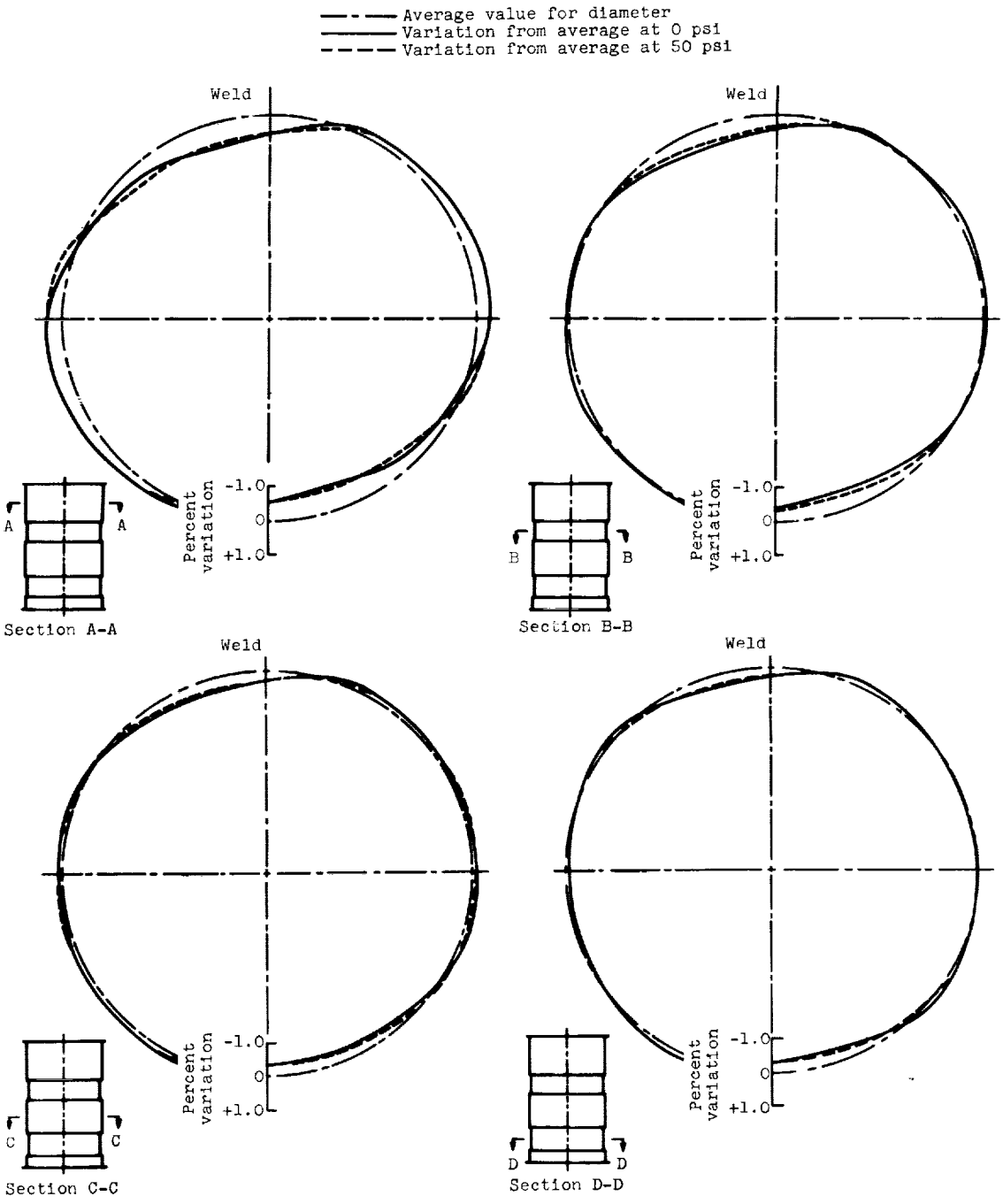

Figure 10. - Results of diameter measurements made on large cylinder at pressures of 0 and 50 pounds per square inch.

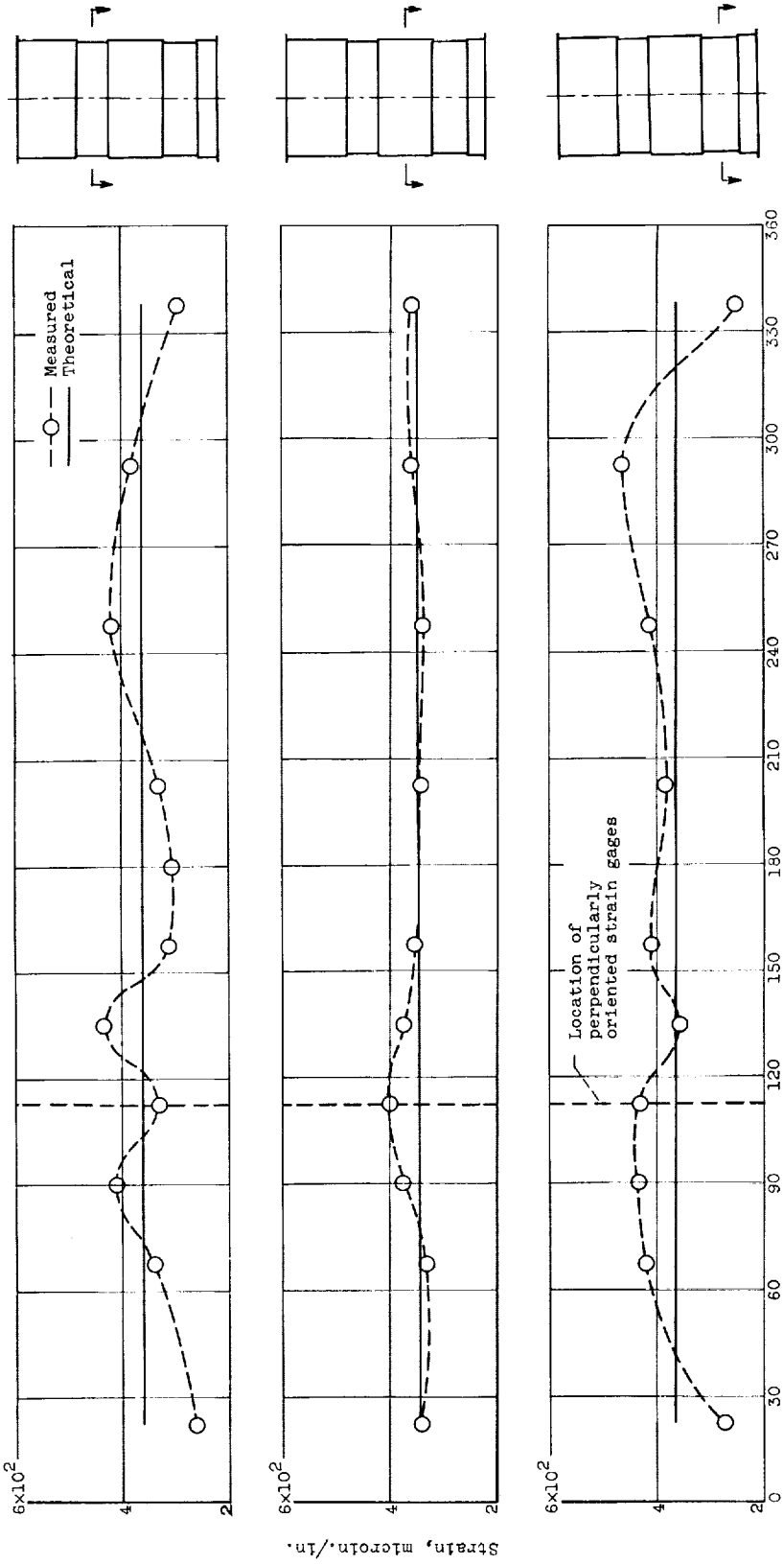

Figure 11. - Meridional strain data from membrane areas in large cylinder. (See fig. 5 for location of strain gages.)

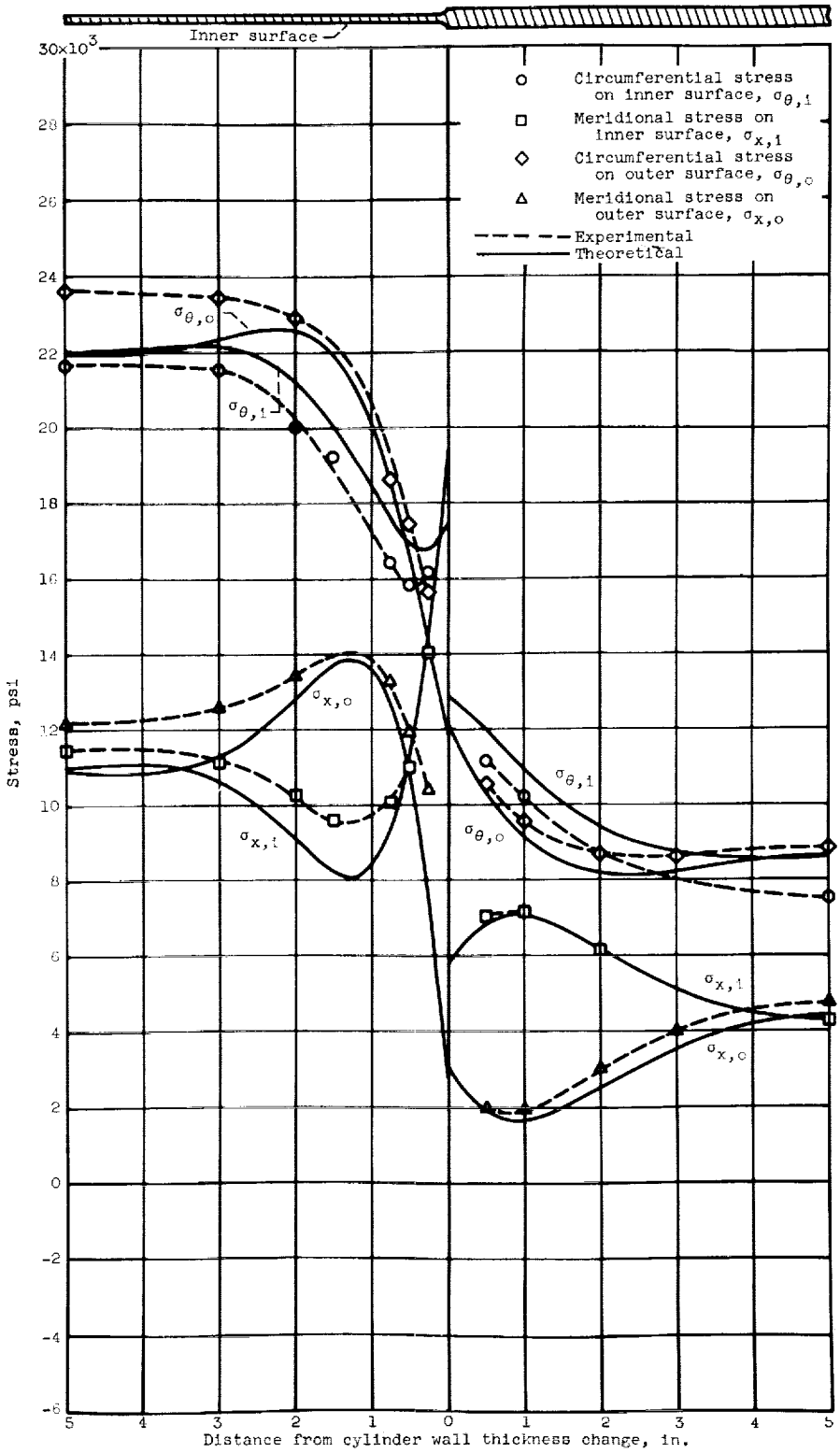

Figure 12. - Comparison between theoretical and experimental stress distribution for large cylinder with continuous middle surface.

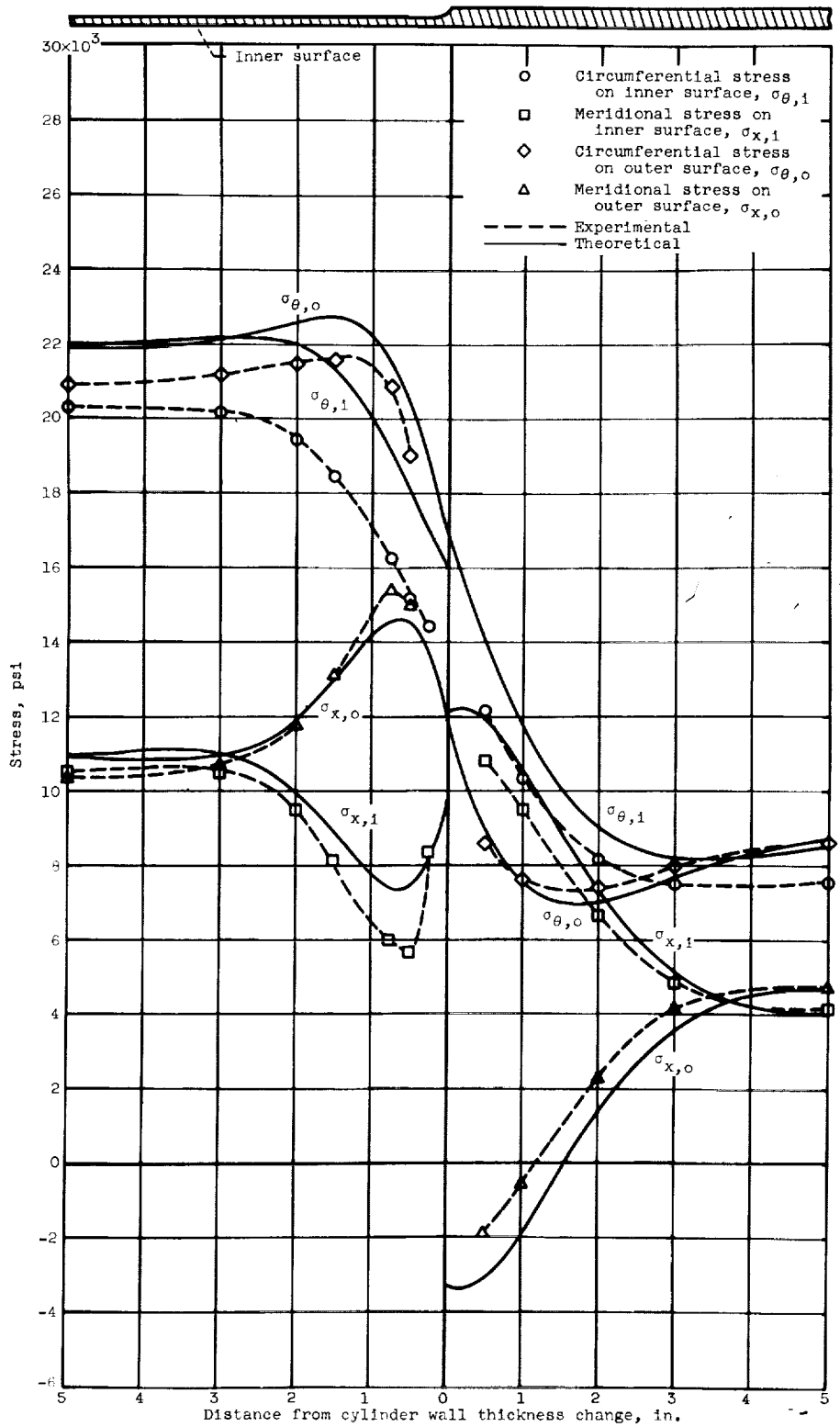

Figure 13. - Comparison between theoretical and experimental stress distribution for large cylinder with continuous inner surface.

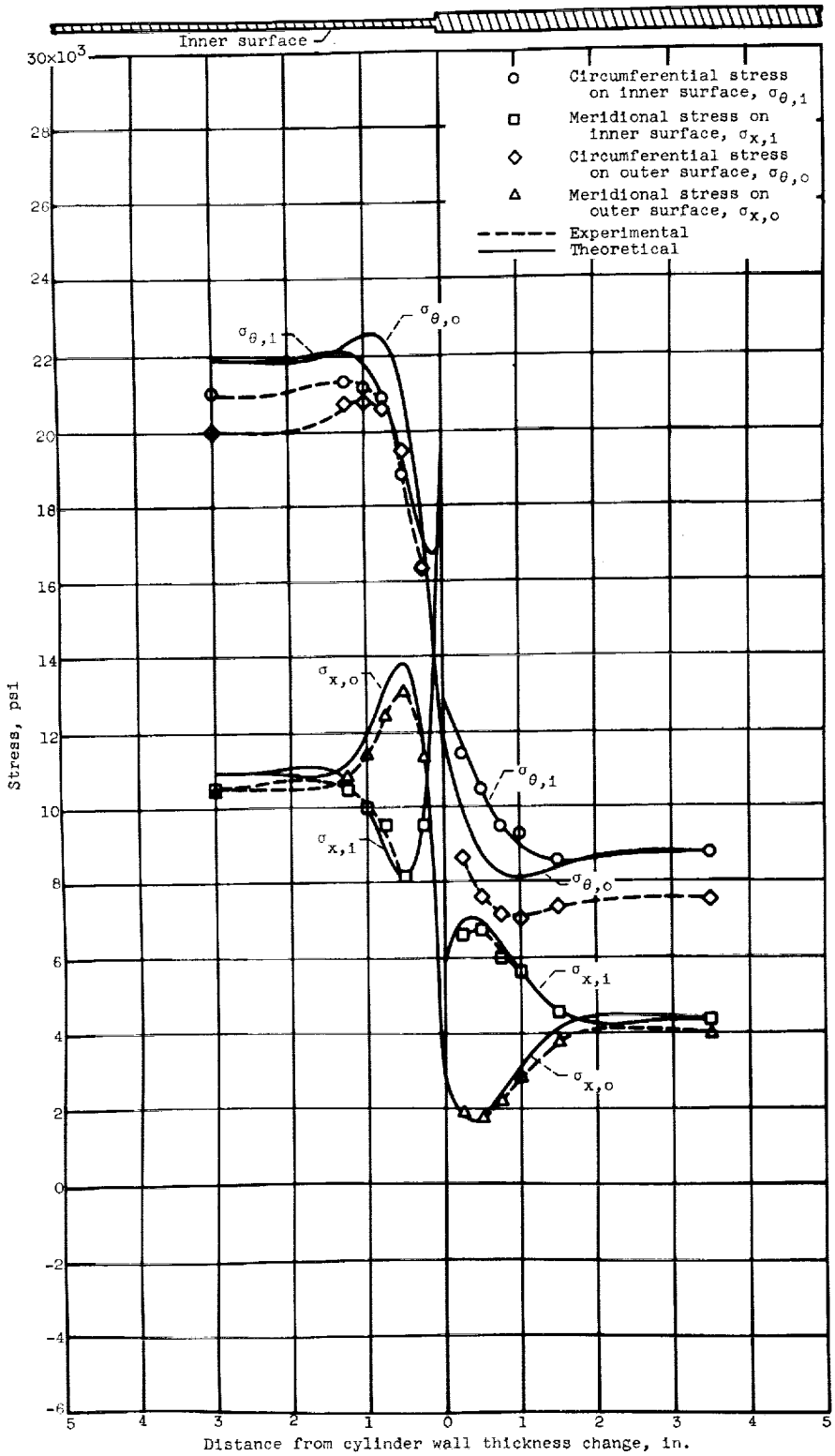

Figure 14. - Comparison between theoretical and experimental stress distribution for small cylinder with continuous middle surface.

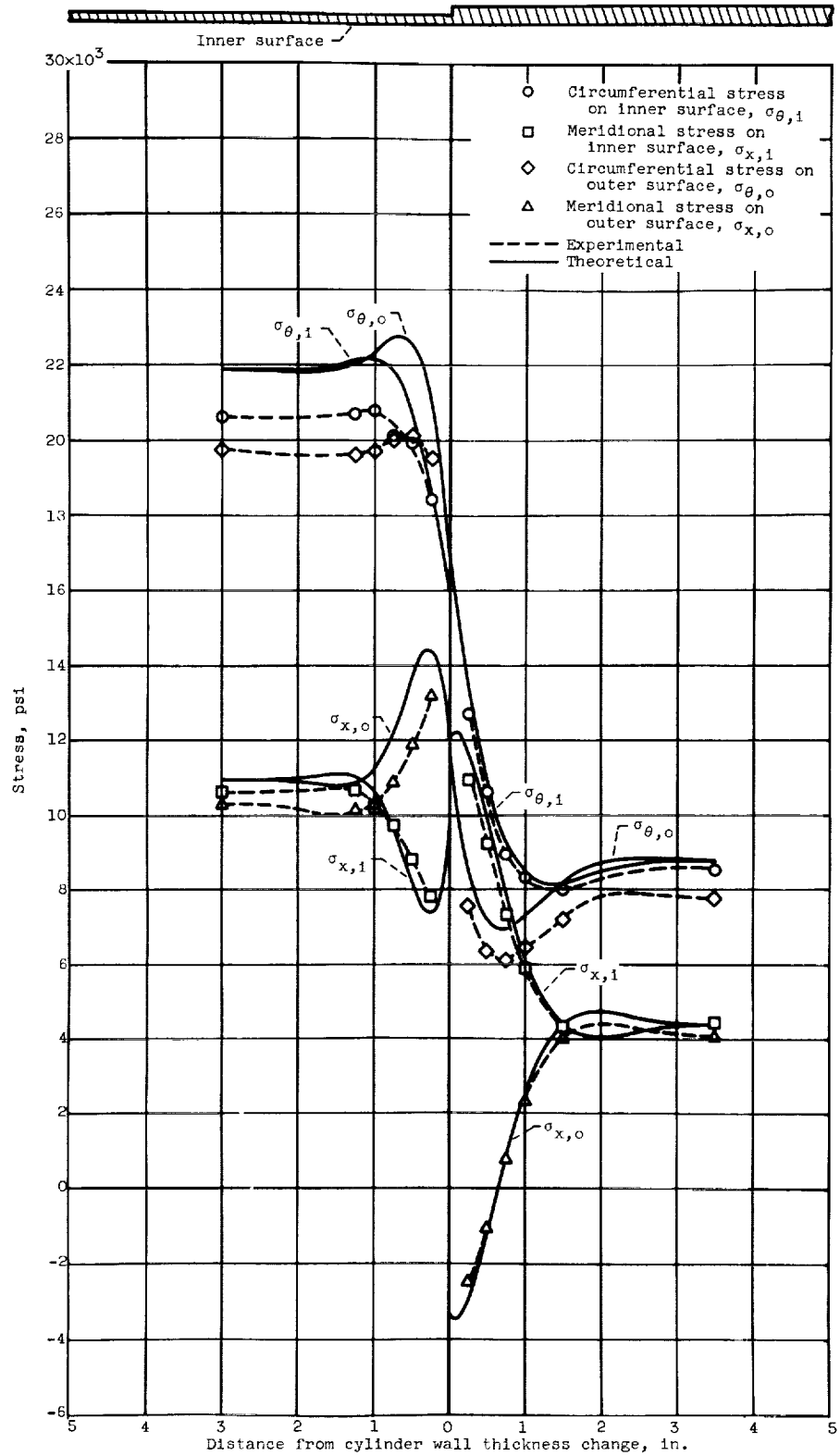

Figure 15. - Comparison between theoretical and experimental stress distribution for small cylinder with continuous inner surface.

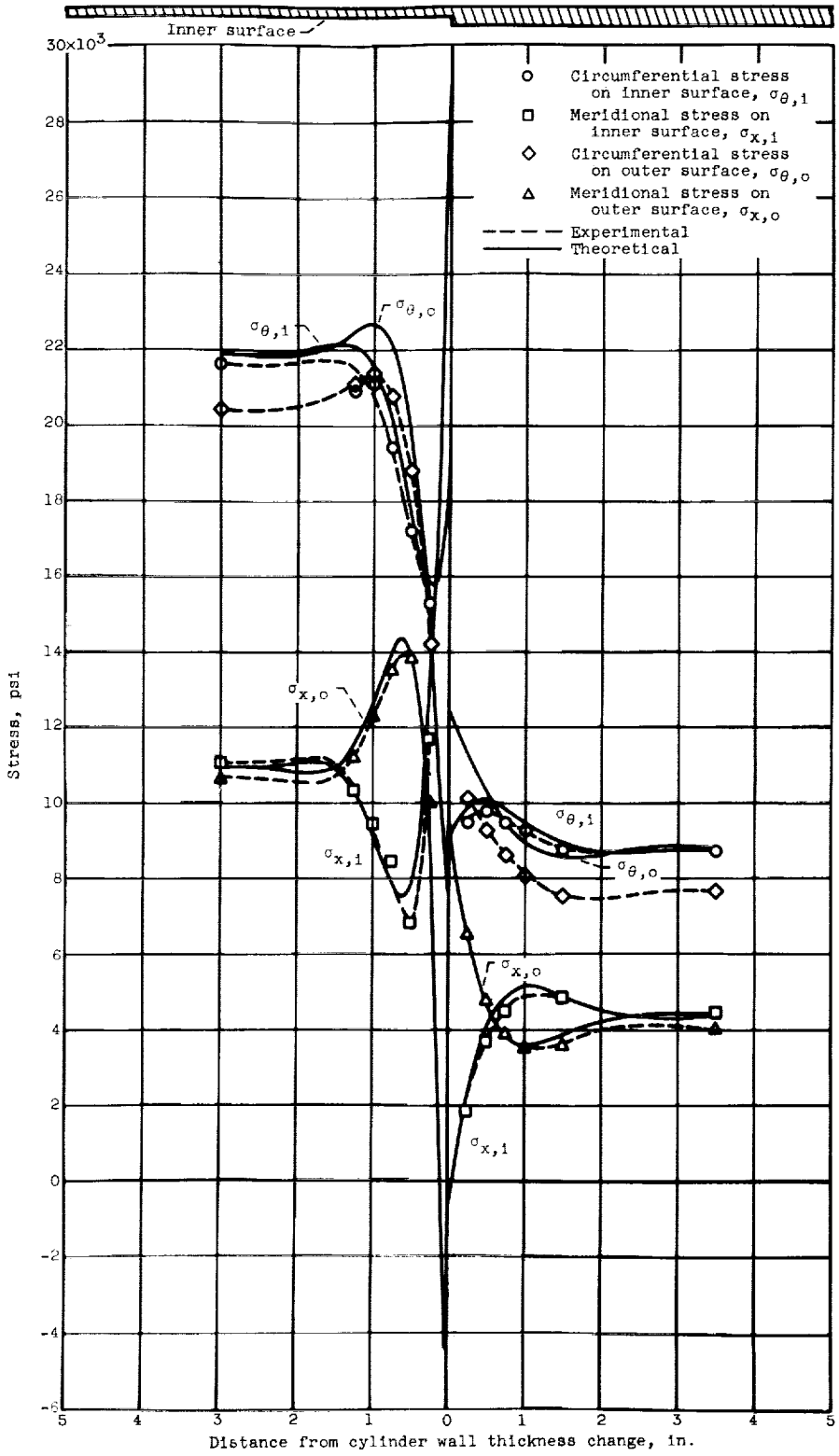

Figure 16. - Comparison between theoretical and experimental stress distribution for small cylinder with continuous outer surface.

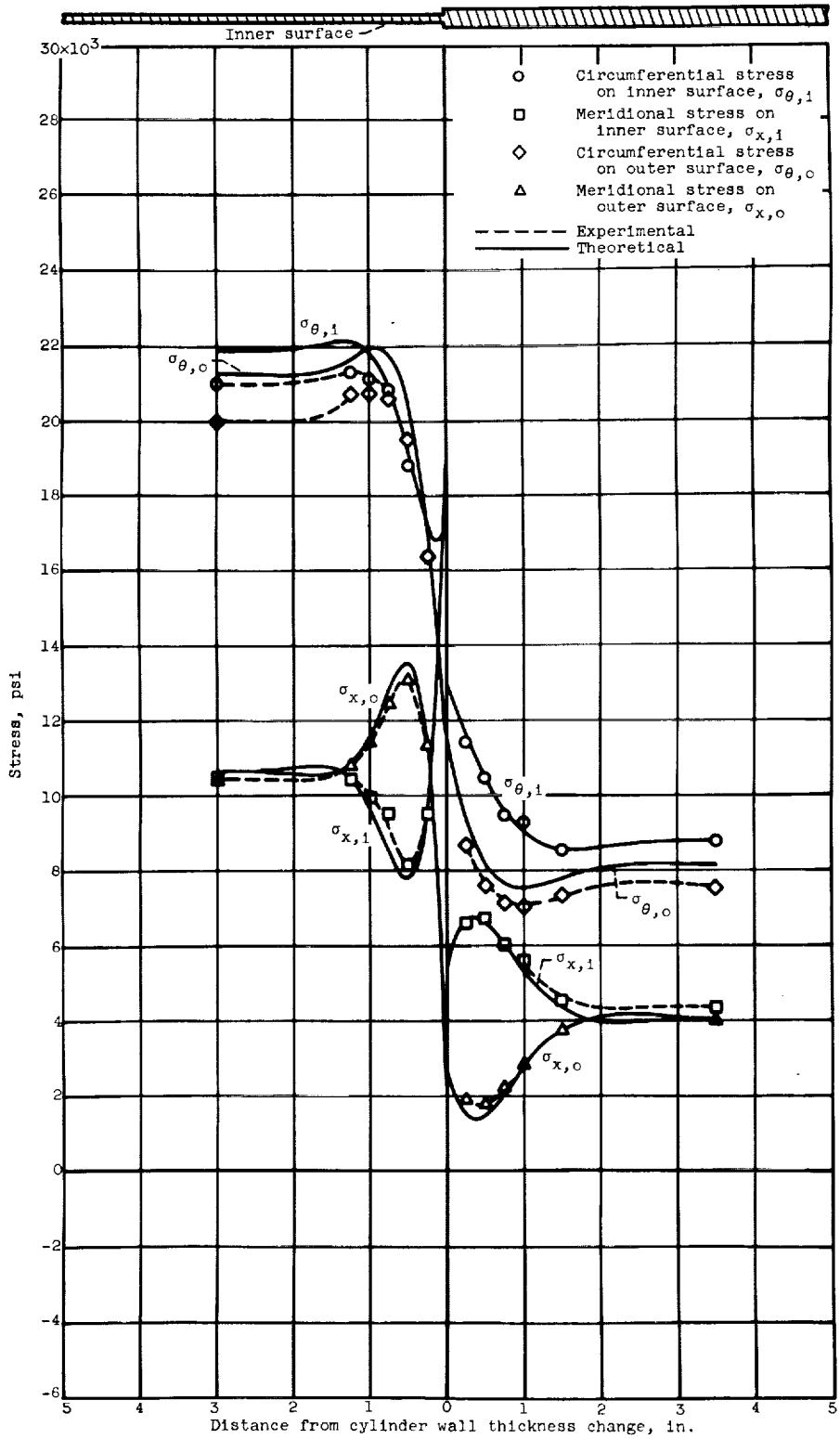

Figure 17. - Modified-calculation comparison between theoretical and experimental stress distribution for small cylinder with continuous middle surface.

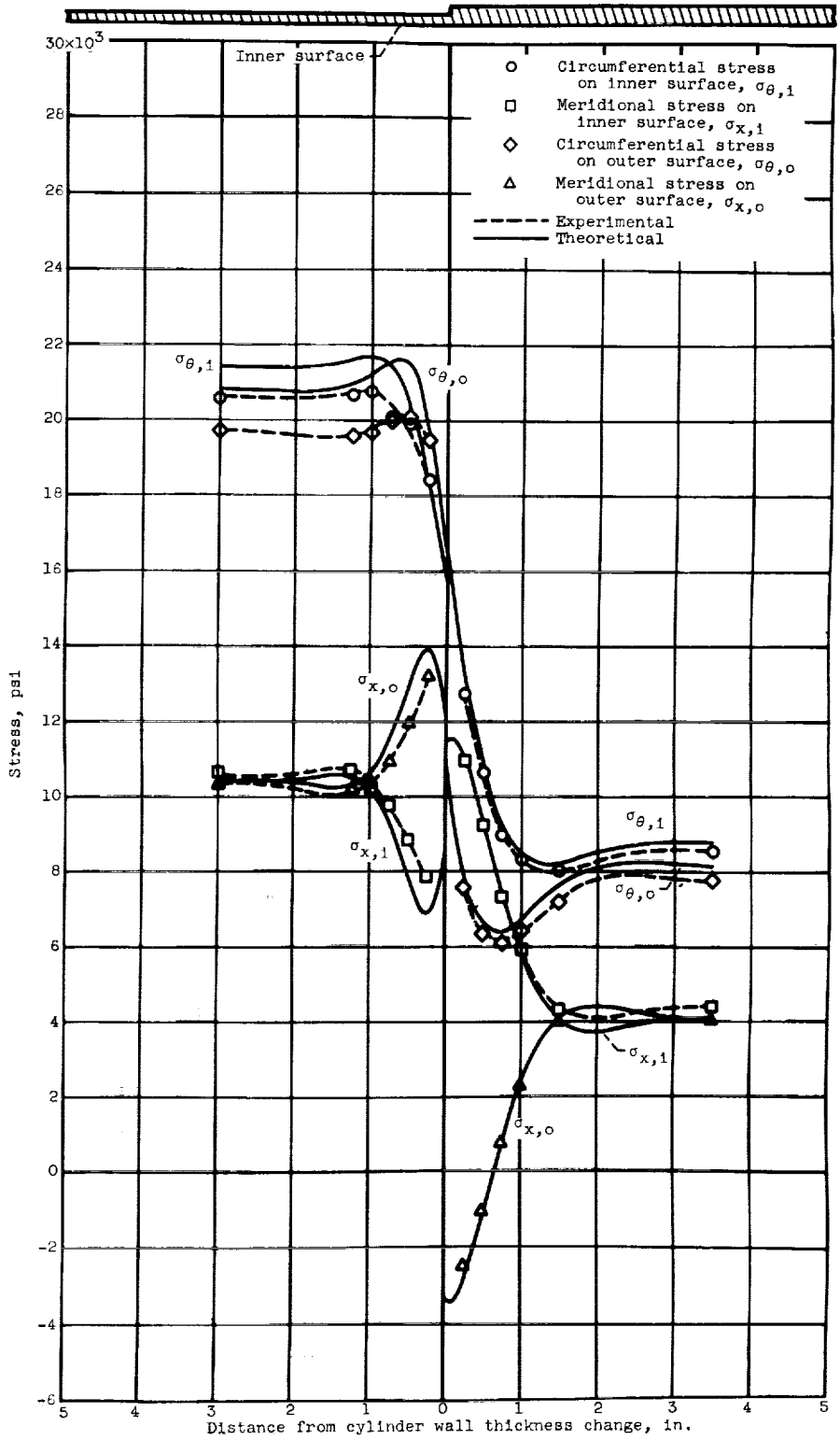

Figure 18. - Modified-calculation comparison between theoretical and experimental stress distribution for small cylinder with continuous inner surface.

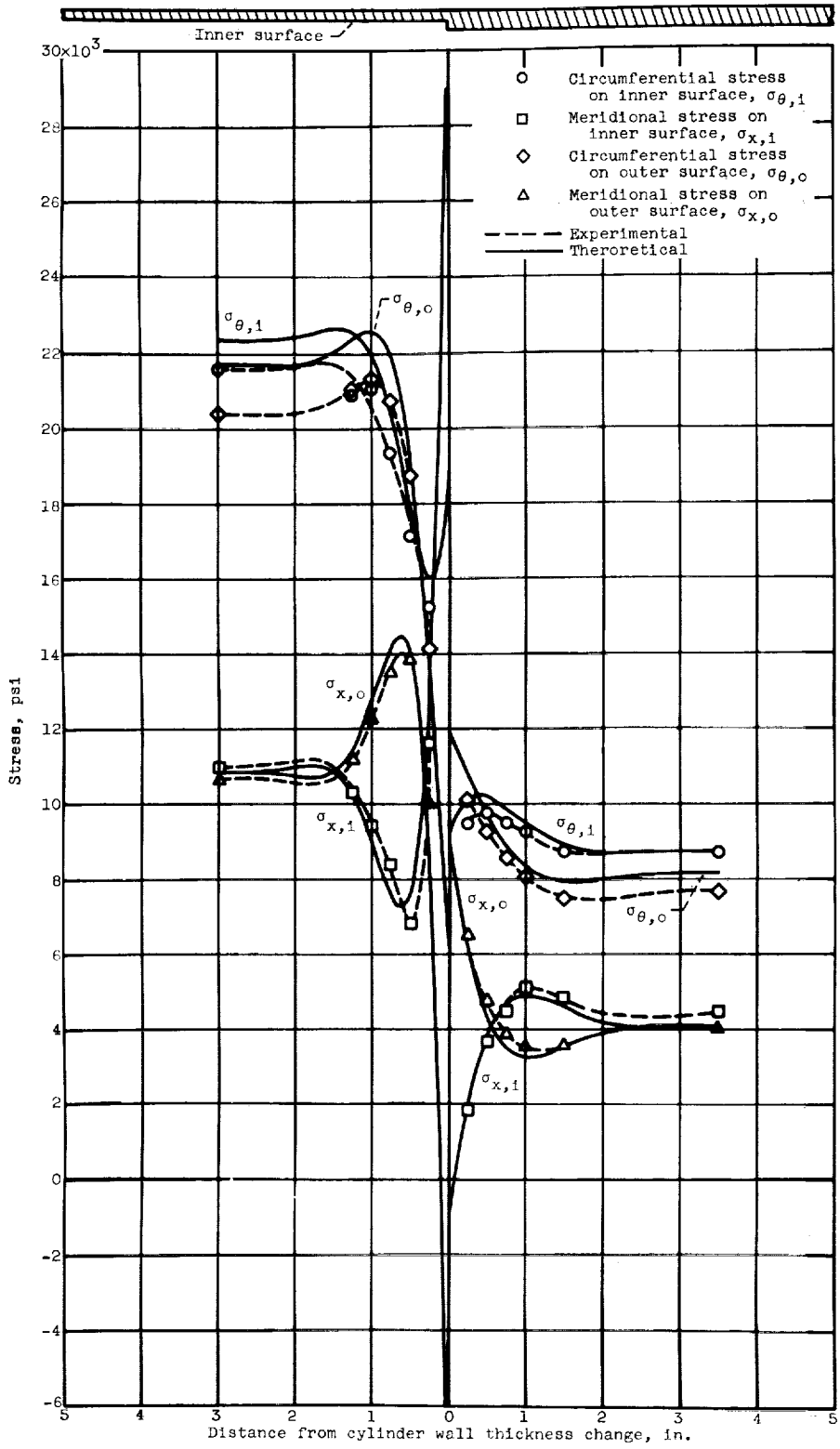

Figure 19. - Modified-calculation comparison between theoretical and experimental stress distribution for small cylinder with continuous outer surface.

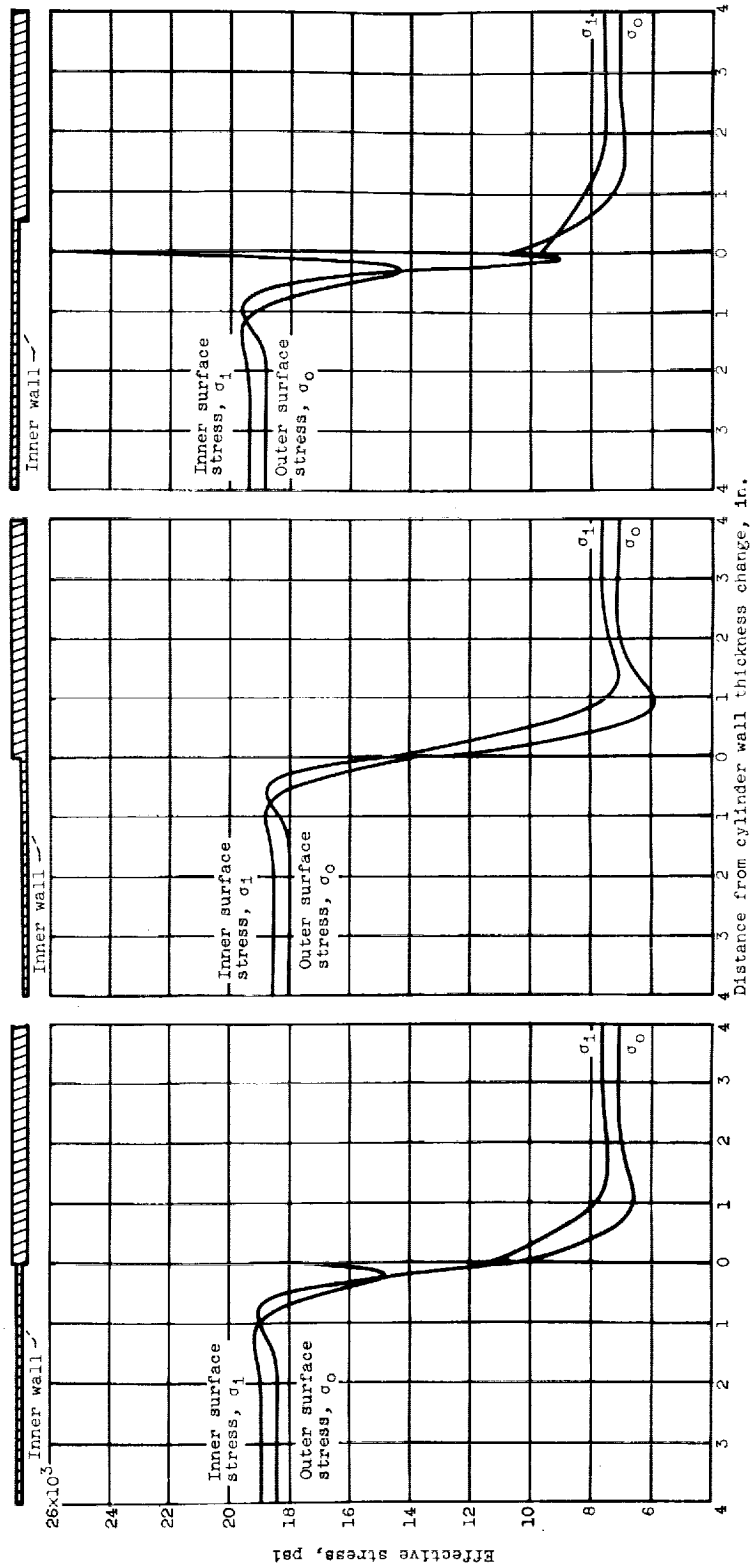

(a) Continuous middle surface (b) Continuous inner surface (c) Continuous outer surface

Figure 20. - Theoretical effective stresses in small cylinder.

E-1508

NASA TN D-1200
National Aeronautics and Space Administration.
EXPERIMENTAL INVESTIGATION OF STRESS DISTRIBUTIONS NEAR ABRUPT CHANGE IN WALL THICKNESS IN THIN-WALLED PRESSURIZED CYLINDERS. William C. Morgan and Peter T. Bizon. June 1962. 40p. OTS price, $1.00. (NASA TECHNICAL NOTE D-1200)

Stress distributions were compared with those predicted by a previously published theoretical method of analysis. This method was developed to include consideration of stresses attributable to differences between average radii in cylindrical sections as well as to thickness changes. Typical cases of radially symmetric abrupt change in cylinder wall thickness were investigated for ratios of diameter to larger wall thickness of 117 and 28. The degree of correlation between predicted and experimental stress distributions established the validity of the theoretical method. The significance of additional stresses caused by change in thickness was evaluated.

I. Morgan, William C.
II. Bizon, Peter T.
III. NASA TN D-1200

(Initial NASA distribution: 24, Launching dynamics; 51, Stresses and loads; 52, Structures.)

NASA

NASA TN D-1200
National Aeronautics and Space Administration.
EXPERIMENTAL INVESTIGATION OF STRESS DISTRIBUTIONS NEAR ABRUPT CHANGE IN WALL THICKNESS IN THIN-WALLED PRESSURIZED CYLINDERS. William C. Morgan and Peter T. Bizon. June 1962. 40p. OTS price, $1.00. (NASA TECHNICAL NOTE D-1200)

Stress distributions were compared with those predicted by a previously published theoretical method of analysis. This method was developed to include consideration of stresses attributable to differences between average radii in cylindrical sections as well as to thickness changes. Typical cases of radially symmetric abrupt change in cylinder wall thickness were investigated for ratios of diameter to larger wall thickness of 117 and 28. The degree of correlation between predicted and experimental stress distributions established the validity of the theoretical method. The significance of additional stresses caused by change in thickness was evaluated.

I. Morgan, William C.
II. Bizon, Peter T.
III. NASA TN D-1200

(Initial NASA distribution: 24, Launching dynamics; 51, Stresses and loads; 52, Structures.)

NASA

NASA TN D-1200
National Aeronautics and Space Administration.
EXPERIMENTAL INVESTIGATION OF STRESS DISTRIBUTIONS NEAR ABRUPT CHANGE IN WALL THICKNESS IN THIN-WALLED PRESSURIZED CYLINDERS. William C. Morgan and Peter T. Bizon. June 1962. 40p. OTS price, $1.00. (NASA TECHNICAL NOTE D-1200)

Stress distributions were compared with those predicted by a previously published theoretical method of analysis. This method was developed to include consideration of stresses attributable to differences between average radii in cylindrical sections as well as to thickness changes. Typical cases of radially symmetric abrupt change in cylinder wall thickness were investigated for ratios of diameter to larger wall thickness of 117 and 28. The degree of correlation between predicted and experimental stress distributions established the validity of the theoretical method. The significance of additional stresses caused by change in thickness was evaluated.

I. Morgan, William C.
II. Bizon, Peter T.
III. NASA TN D-1200

(Initial NASA distribution: 24, Launching dynamics; 51, Stresses and loads; 52, Structures.)

NASA

NASA TN D-1200
National Aeronautics and Space Administration.
EXPERIMENTAL INVESTIGATION OF STRESS DISTRIBUTIONS NEAR ABRUPT CHANGE IN WALL THICKNESS IN THIN-WALLED PRESSURIZED CYLINDERS. William C. Morgan and Peter T. Bizon. June 1962. 40p. OTS price, $1.00. (NASA TECHNICAL NOTE D-1200)

Stress distributions were compared with those predicted by a previously published theoretical method of analysis. This method was developed to include consideration of stresses attributable to differences between average radii in cylindrical sections as well as to thickness changes. Typical cases of radially symmetric abrupt change in cylinder wall thickness were investigated for ratios of diameter to larger wall thickness of 117 and 28. The degree of correlation between predicted and experimental stress distributions established the validity of the theoretical method. The significance of additional stresses caused by change in thickness was evaluated.

I. Morgan, William C.
II. Bizon, Peter T.
III. NASA TN D-1200

(Initial NASA distribution: 24, Launching dynamics; 51, Stresses and loads; 52, Structures.)

NASA